THEORY OF DROPLET: I
RENORMALIZED LAWS OF DROPLET
VAPORIZATION IN NON-DILUTE SPRAYS

H.H. CHIU
Department of Mechanical Engineering
The University of Illinois at Chicago
Chicago, Illinois 60680

ABSTRACT

The vaporization of a droplet, interacting with its neighbors in a non-dilute spray environment is examined as well as a vaporization scaling law established on the basis of a recently developed theory of renormalized droplet.[1] The interacting droplet consists of a centrally located droplet and its vapor bubble which is surrounded by a cloud of droplets. The distribution of the droplets and the size of cloud are characterized by a pair-distribution function. The vaporization of a droplet is retarded by the collective thermal quenching, vapor concentration accumulated in outer sphere, and by the limited percolative passages for mass, momentum and energy fluxes. The retardation is scaled by the local collective interaction parameters; group combustion number of renormalized droplet, droplet spacing, renormalization number and the local ambient conditions. The numerical results of a selected case study reveal that the vaporization correction factor falls from unity monotonically as the group combustion number increases, and saturation is likely to occur when the group combustion number reaches 35-40 with interdroplet spacing of 7.5 diameters and the environment temperature of 500 K. The scaling law suggests that dense sprays can be classified into: (1) a "Diffusively Dense" cloud characterized by uniform thermal quenching in the cloud, (2) a "Stratified Dense" cloud characterized by a radial stratification in temperature by the

differential thermal quenching of the cloud, or (3) a "Sharply Dense" cloud marked by fine structure in the quasi-droplet cloud and the corresponding variation in the correction factor due to the variation in the topological structure of the cloud characterized by pair-distribution function of quasi-droplets.

NOMENCLATURE

D	Mass diffusion coefficient
g	Pair – distribution function
G	Group combustion number
L	Latent Heat of vaporization
$\dot{m}$	Vaporization rate
n	Number density
q	Heat of combustion
r	Radial coordinate
R	Radius
s	Droplet separation
T	Temperature
υ	Velocity
W	Molecular weight
α	Schvab-Zeldovich Variable
β	Renormalization number n_{ts}/n_{co}
γ_F	L/q
ε_F	$-(W_F \nu_F)^{-1}$
θ	$r_\ell(\eta)/r_\ell(o)$
ν	Stoichiometric coefficient
η	r/r_ℓ
ρ	Density

Subscript

c   Canonical bubble

co   Canonical bubble of test droplet

F   Fuel

T   Temperature

ℓ Liquid drop surface

ts   Transition sphere surface

1. Introduction

Increasing theoretical findings [1-13] and experimental evidence [14-18] attest the widely held belief that the short-range collective interaction [2-6], [11-13] among the neighboring droplets and the long-range interaction [1, 7, 9], [10] with the droplets at distance, on a hydrodynamic scale, have profound impact on the state of a droplet, i.e. the states of saturation, vaporization, ignition, combustion and extinction, as well as the droplet interfacial process rates in non-dilute cloud or spray environments. These collective interactions, produced by local hydrodynamic and transport processes in a complex topological environment, serve to control the percolative passage for dispersing mass, momentum energy fluxes and the effective interfacial area for the property exchange processes. These interactions result in the collective thermal quenching, the accumulation of vaporizing species and the tendency for stagnating the microscale local Stefan flow and mean flow through dynamic equilibration between the two phases.

Review of the current theories of collective interactions including: Group Vaporization and Combustion [1, 7, 10] (GVC), Discrete Droplet Model (DDM) [2, 3, 5] and Droplet In Bubble (DIB) [4, 8] reveals two major theoretical deficiencies in the theory of short-range interaction and droplet rate processes at this juncture. These are: (1) the lack of the fundamental concepts and the mechanisms interlinking small scale discrete droplet processes with a large scale quasi-continuum flow of a non-dilute cloud or a spray, and (2) the incomplete understanding of complex interfacial processes, finite rate reaction, turbulence and transport processes that occur in the vicinity of each droplet. The first issue compels the current research of non-dilute sprays to proceed with two rival approaches; GVC, that primarily

68

deals with the long-range interaction, thus neglecting small scale resolution, and DDM, which focuses attention on the detailed behavior of discrete droplets in well-ordered droplet assemblies, thereby requiring a laborious computational procedure involving a large number of droplets encountered in practical sprays.

The alternative approach, adopting a continuous spray model supplemented by realistic droplet laws, appears the compromised mean of the prediction of non-dilute spray. A recent study of Tishkoff [4] on the numerically correlated vaporization correction factor derived from the DIB model demonstrates the viability of such combined approach to complement modern non-dilute spray calculations formulated on either Eulerian-Eulerian or Eulerian-Lagrangian framework. It must be mentioned, however, that an attempt to deduce an improved droplet vaporization law from the results of existing DDM met with difficulties due to the geniune lack of a self-consistent criterion of "droplet environment" whereupon the gas properties such as the temperature and concentration of vapor species, are inserted in the droplet law for the determination of the vaporization rates. A universal theory of short-range interaction and a set of comprehensive laws of droplet rate processes remain as the major unsolved issues in the contemporary theory of non-dilute sprays which has been the central theme of research [12, 13] conducted. The objectives of this paper are to present the basic concepts, theoretical approaches and the results of Renormalized Droplet (RND) theory to establish vaporization laws for droplets in a stationary non-dilute cloud environment.

The paper begins with the descriptions of droplet models and theories, in section 2, to clarify basic concepts and definitions of "droplet," adopted in modern spray theory. The structure, model and mathematical analysis of RND

are described in Section 3. The results of numerically predicted RND structure, vaporization correction factor and their dependence on collective interactive parameters are presented in Section 4.

2. Droplet Models: Topological Properties and Modeling

2.1 Elemental Model

Three fundamental topological properties that play basic roles in interaction phenomena between the droplet under investigation, termed the "test droplet", and its neighbors, i.e. "field droplets," are; (1) "graininess" or "discreteness" of a droplet, (2) "covolume" or "evacuated volume" of a droplet, and (3) "localization" of a droplet relative to a reference point. Basic droplet models which attempt to capture properties of the droplet to a desired level of accuracy, are classified into three types according to the level of sophistication in the characterization of the topological features, as summarized in Table 1. First, the "natural droplet model" which characterizes a droplet by its true geometrical shape, size and location, simulates all the topological properties described above.

Table 1
Droplet Models

Droplet Properties	Natural Drop Model	Quasi-Droplet Model		
		Non-Uniformly Smeared Drop	Uniformly Sheared Drop	Point Source Model
Graininess	Sharp*	Diffuse**	No	Singular
Covolume	Sharp	No	No	No
Localization	Sharp	Diffuse	No	Singular

*Sharp properties caused by phase discontinuity
**Diffuse properties featured by the absence of phase discontinuity

The natural droplet model provides a sharp droplet configuration required for the predictions of microscale flow structure, and results from a combination of convective and Stefan flows, and interfacial process rates of the test droplet. The solution is given by solving Dirichelt boundary value problems associated with conservation equations and a well defined set of physical boundaries formed by the interface of droplets.

The second type of model, i.e. "quasi-smeared droplet," describes a droplet by a medium spreading through the space. The droplet thus coexists with the host medium without apparent phase discontinuity. The models in this category are further divided into "uniformly" and "non-uniformly" smeared droplets, Fig. 1. In the latter model, the location and spatial extension of droplets are depicted by a joint probability distribution function. The "graininess" and "localization" of droplets are therefore partially characterized by the joint probability function rather than the phase discontinuities as in the case of the natural drop model.

"The uniformly smeared droplet model" which has been adopted in the majority of two-phase flow and spray theories is a special case with a uniform distribution of the joint probability with its numerical value equals to unity throughout the space. In this model, "graininess" and "localization," are

absent. Because of the lack of the basic topological properties, these quasi-droplet models are unable to be used for the determination of the droplet bound flow field and droplet laws. However, when appropriate droplet laws are provided to describe the interfacial processes rates, the flow structure of a farfield can be predicted with an acceptable accuracy by a quasi-two phase approach that is simpler than the Dirichelt boundary value problems.

The third model is a "point source model" which uses a mathematical singularity to characterize the "location" and a "singular graininess" of a droplet in a dilute spray with a large spacing, i.e., the ratio of spacing to the droplet size is much greater than unity. Like a "quasi-droplet model", the "point source model" fails to provide a satisfactory near-field structure required for the prediction of the rates of interfacial processes, but the model offers a simple mathematical theory for the prediction of far field solutions.

2.1.2 Composite Model

Although a specific elemental model has been frequently used in the analysis of single droplet, or many-droplet problems (e.g. natural droplet model in DDM and DIB, uniformly smeared droplet in GVC), the potential advantages of the simultaneous use of two or more than two elemental models has not been fully exploited.

A composite modeling technique permits a strategic selection of a desired elemental model in a certain selected region and an alternative model in another region to enhance the modeling flexibility and the simplicity in analysis. The choice of an elemental model is determined by the type of the flow field data and accuracy required in each region. For example in RND

theory, the test droplet is modeled by a "natural droplet model" to facilitate the determination of the near flow field, which depends on the detailed geometry of the test droplet, and the flow disturbance created by the neighboring field droplets. On the other hand, "field droplets" are modeled by "non-uniformly smeared droplet" which are distributed in the neighborhood of the test droplet. The distribution of these quasi-droplets is described by a joint probability function to simulate localization and graininess of the quasi-droplets. This composite model provides a simple, self-consistent and useful analytical method of treating the interfacial phenomena of a test droplet interacting with its neighbors. The details of the application of composite model in RND is described in the remaining part of this section and the next section.

2.2 Theories of Droplet: Canonical and Renormalized Representation of a Droplet Under Short Range Interaction.

"The Theory of Droplet" concerns itself with interfacial phenomena and the process rates of a test droplet in isolation or under the influence of the collective interaction of field droplets. A representative analytical approach for the former is the single droplet theory, and for the latter case, the approaches are DIB and RND models. Since the latter problem concerns collective interaction between a test droplet and field droplets, the nature of the problems and the theoretical procedures are, in general, similar to that of "many droplet problems". However, an important distinction between the two theories is that the "droplet theory" aims to establish the rate of an interfacial process of a test droplet on the framework of "the minimum-sized many-droplet system" that includes the smallest number, N_{min}, of droplets

73

i.e., a test droplet and $N_{min}-1$ field droplets confined in, "the minimum sized region", i.e. R_{min} region. The requirements of "the minimum number of droplets" in "the minimum region" are imposed in RND theory so that the droplet laws, deduced from such a minimum droplet system, can be explicitly formulated in terms of the self-consistently defined "local properties" of a spray flow field. This basic feature of "local representation," is essential in modern spray calculations that use local droplet laws. In contrast to the theory of renormalized droplet, the "cluster" model[8,11] treats a droplet system with an arbitrary number of droplets in a finite region. Thus, the model is appropriate for dealing with a partial or complete domain of a spray by an approach that is different from the conventional spray theory.

2.2.1 Canonical Droplet Theory[4]: CDT

The DIB[4] which consists of a natural droplet and its Wigner-Seitz bubble, has two fundamental properties. Firstly, a high degree of symmetry preserved in the DIB's periodical droplet assembly inhibits the transports of mass, momentum and energy transports among the neighbor droplets. Thus, DIB portrays a thermo-chemically closed adiabatic system with respect to neighbor droplets. Secondly, the strength of the interaction between the droplet and its bubble is determined by the size of the bubble which has the radius equals to half of the droplet spacing. When the droplet separation becomes infinitely large, the predicted vaporization rate approaches to that of an isolated droplet, as expected.

Because of these two unique features of the DIB which may be regarded as a reference model of a short-range interaction, the theory will be termed "canonical droplet theory" (CDT). The theory provides a basis of RND model described in the following subsection.

74

2.2.2   Renormalized Droplet Theory

Since the canonical theory treats the interfacial processes of a droplet in a hypothetical, well ordered droplet lattice, the validity of the canonical droplet law is questionable when applied to practical sprays with disordered droplet distributions. Needless to say, the adiabaticity and closure of the test droplet relative to its neighbor also break down in practical sprays. Another theoretical deficiency of DIB is the lack of the geometrical compatibility of the "environment" with that of droplet environment in spray theory. In CDT, the edge of a bubble has been adopted as the environment, though such choice is not necessarily the unique alternative, and the gas temperature or species concentration is used for the determination of the vaporization rate and droplet transient heating rate. However, in a spray calculation, the local average gas phase temperature of multi-phase flow is used for the determination of droplet process rates. Clearly, the environment of a canonical droplet does not coincide with that of a spray. Such incompatibility prohibits the encoding of the droplet law, derived by DIB, into a spray calculation unless an explicit link between two environmental properties, i.e., DIB vs smeared droplet model adopted in a conventional multi-phase continuum spray is provided.

The RND theory provides a rigorous theoretical procedure that removes the major shortcomings of the canonical theory and provides encodable droplet laws by the applications of (1) composite droplet modeling technique and (2) the minimum sized many-droplet system, as described in the following section.

3. Renormalized Droplet (RND)

3.1 Structure of Model

The theory of renormalization[12] portrays a test droplet interacting with its neighboring field droplets by a composite "dressed or clothed" droplet model shown in Fig. 2. Two principal structural elements of RND are (1) a Droplet-In-Bubble (DIB) and (2) a cloud of non-uniformly smeared droplets which functions as an external clothing for the DIB. The distribution of the quasi-droplet is described by the pair-distribution function representing the joint probabiltiy of finding a test droplet and its neighbor at a separation s. The pair-distribution function vanishes in the immediate vincinity of the bubble, representing the evacuated volume effect of droplets, and then increases rather rapidly to a value greater than unity at the radial distance comparable to a mean droplet spacing. This first high droplet density region populated by the nearest neighbor droplets is termed the "first coordination shell." The population peaks of the "second and higher order coordination shells" lose their sharpness as they merge with one another and are ultimately lost in a continuous environment where the pair distribution function approaches to unity. The size of the transition sphere, R_{ts}, defined as the radial location where the pair distribution function is 0.99, depends on the droplet size, spacing and arrangement. The ratio of the size of the transition sphere, R_{ts}, to the characteristic hydrodynamic scale, L, is typically much smaller than unity, and thus the sphere degenerates into a point in the limit when R_{ts}/L vanishes. Accordingly, the average properties of the gas over the transition sphere approach to the local properties of the continuum flow as the limit R_{ts}/L goes to zero. This "correspondence hypothesis" and the interlinking transition sphere constitute the two key

76

factors for the determination of the droplet process rate by the local gas properties of the continuum flow field. In the present analysis, RND is assumed to be spherically symmetric, and non-reacting. Transport properties are constant and the Lewis number is unity.

The criterion of a quasi-steady state is a much more complex issue than that of a single droplet because of the multi-scale and multi-time phenomena linked with mass and energy transport in typical RND. In general, the quasi-steady state assumption is valid when (1) the largest characteristic diffusion and conduction times associated with the transition sphere is much smaller than the life time of any droplet in the cloud, (2) no droplet in the transition sphere is in the state of transient heating, and (3) no gas phase region is experiencing an initial or a terminal transient process. The effects of transient processes, and the validity or the limitation of the quasi-steady theory in a practical spray are discussed in Section 5. Detailed time-dependent analysis of transient processes in RND, which will be presented as Part II in the future, reveal that RND is found in some dense sprays to exhibit only a brief or finite period of quasi-equilibrium state. Additionally, RND exhibits dynamic saturation in time scales comparable to the characteristic diffusion time in the canonical bubble when the local group combustion number exceeds a critical value.

3.2 Mathematical Analysis

Non-dimensional equations governing RND are formulated separately for the inner DIB region and an external quasi-droplet cloud, respectively, as follows.

$$\frac{1}{\eta^2} \frac{d}{d\eta} \left(\eta^2 \frac{d\psi_i}{d\eta} \right) = 0 \qquad\qquad 1 \leq \eta \leq \eta_{co} \qquad\qquad (1)$$

and

$$\frac{1}{\eta^2} \frac{d}{d\eta} (\eta^2 \frac{d\hat{\psi}_i}{d\eta}) = G_s g\mu \hat{B}_i \qquad\qquad \eta_{co} \leq \eta \leq \eta_{ts} \qquad (2)$$

with

$$\psi_m = \rho\upsilon \qquad\qquad\qquad (3)$$

$$\begin{pmatrix} \psi_F \\ \psi_T \end{pmatrix} = \psi_m \begin{pmatrix} \alpha_F \\ \alpha_T \end{pmatrix} - \sigma \frac{d}{d\eta} \begin{pmatrix} \alpha_F \\ \alpha_T \end{pmatrix} \qquad\qquad (4)$$

where $\eta = r/r_\ell(0)$, ρ and v are non-dimensionalized by the gas density, and velocity on the droplet surface, respectively, $Gs = 4\pi n r_{\ell,o}^3$, g is a pair distribution function, μ is the vaporization shape factor defined by (12), ψ_i are the fluxes of various properties; mass for $i = m$, fuel vapor for $i=F$ and thermal energy for $i=T$, and $\hat{}$ refers to the properties pertaining to an outer region. The definitions of properties α_i and constants B_i are summarized in Table 2.

Table 2
Schvab-Zeldovichs Variables and Constants

i	α_i	$\hat{\alpha}_i$	$\hat{B}_i$
M	$-(y_f/W_F\nu_F)$	$\int_F^T/W_F\nu_F)$	$\varepsilon_F = -(W_F\nu_F)^{-1}$
T	$\int_{T_b}^T C_p dT/q$	$\int_{T_b}^T \hat{C}_p \hat{T} dT/q$	$\gamma_F = L/q$

The system of Eqs. (1)-(4) is integrated by a repeated quadrature. The constants of integration are determined from the conditions of the

impermeability of the gaseous species on the droplet surface and the balance of the heat conducted to the droplet with the latent heat of the vaporization. The integration gives the following vaporization laws

$$\dot{m}(0) = \frac{4\pi\rho D r_\ell(o)\, \ell n\left(1 + \frac{\alpha_{Tco}}{\gamma_F}\right)}{1 - \zeta_{co}} \tag{5}$$

or

$$\dot{m}(o) = \frac{r\pi\rho D r_\ell(o)\, \ell n\left(1 + \frac{\alpha_{Fco} - \alpha_{F\ell}}{\alpha_{F\ell} - \epsilon_F}\right)}{1 - \zeta_{co}} \tag{6}$$

where

$$\zeta_{co} = \eta_{co}^{-1}$$

These laws, which agree with those obtained by Tishkoff[4], are valid for any value of ζ_{co}, provided the bubble contains no droplet other than the test droplet. This standard law will be termed "canonical vaporization law," the spherical bubble surface will be identified by "canonical environment" and the bubble temperature by "canonical temperature." In contrast to what is described above, an alternative law in which the vaporization rate is determined by the gas temperature on the surface of the transition sphere (see Fig. 2) will be called "renormalized vaporization law," the surface of transition sphere is "renormalized environment" and temperature on the surface is the "renormalized temperature" which is numerically equal to the local gas temperature of the continuum flow field.

Renormalized Droplet Law

Since the continuum theory of sprays predicts the local gas temperature but not the canonical temperature, the canonical vaporization laws (5) and (6) cannot be used in spray calculation as previously described. The alternative proposed in this paper is to use a renormalized vaporization law. The renormalized law is described in this subsection. By adopting a mathematical procedure involving appropriate linear combinations of Eq. (2) governing ψ_m, ψ_F and ψ_T, one obtains two homogeneous equations governing $\hat{\alpha}_T + \gamma_F$ and $\hat{\alpha}_F - \epsilon_F$. These two equations are integrated and joined with the inner solutions on the surface of the canonical bubble. The resulting solutions are given by

$$\frac{\hat{\alpha}_T + \gamma_F}{\hat{\alpha}_{Tts} + \gamma_F} = \frac{\hat{\alpha}_F - \epsilon_F}{\hat{\alpha}_{Fts} - \epsilon_F}$$

$$= \exp\left\{ -\frac{1}{\sigma} \int_{\eta}^{\eta_{ts}} \frac{1}{\eta^2} \left(1 + G_s \int_{\eta_{co}}^{\xi^2} g\mu\xi^2 d\xi \right) d\eta' \right\} \tag{7}$$

In order to obtain the renormalization laws, one first determines $\hat{\alpha}_{Tco}$ and $\hat{\alpha}_{Fco}$ by replacing the η appearing in the lower limit of the integration of Eq. (7) by η_{co}. Subsequently, by substituting the resulting expressions of $\hat{\alpha}_{Tco}$ and $\hat{\alpha}_{Fco}$ in Eq. (5) and (6) one arrives at the following renormalized vaporization laws:

$$\dot{m}(o) = 4\pi\rho Dr_\ell(o) C_v \ln\left(1 + \frac{\hat{\alpha}_{Tts}}{\gamma F}\right) \tag{8}$$

$$\dot{m}(o) = 4\pi\rho Dr_\ell(o) C_v \ln\left(1 + \frac{\hat{\alpha}_{Fts} - \hat{\alpha}_{F\ell}}{\hat{\alpha}_{F\ell} - \epsilon_F}\right) \tag{9}$$

80

where C_v is the vaporization correction factor calculated as follows

$$C_v = [\ 1 - \zeta_{ts} + G_s \int_{\eta_{co}}^{\eta_{ts}} \int_{\eta_{co}}^{\eta} K(\eta|\xi)\mu(\xi)d\xi d\eta]^{-1} \qquad (10)$$

in which

$$K(\eta|\xi) = \eta^{-2} \xi^2 g(\xi) \qquad (11)$$

$$\mu = \frac{\dot{m}(\eta)}{\dot{m}(o)} = \frac{4\pi\rho D r_\ell \ln[1+\dfrac{\hat{\alpha}_{Tc}(\eta)}{\gamma_F}]}{\dot{m}(o) \ [1-\zeta_c (\eta)]} \qquad (12)$$

where $\alpha_{F\ell}$ is given by

$$\alpha_{F\ell} = \frac{\hat{\alpha}_{Fts} + \hat{\alpha}_{Tts} + \varepsilon_F}{\hat{\alpha}_{Tts} + \gamma_F} \qquad (13)$$

The vaporization laws (8) and (9) remain incomplete until the distribution of μ is provided. The determination of μ requires the knowledge of the canonical temperature $\hat{\alpha}_{Tc}(\eta)$ of a quasi-droplet located at η, see Eq. (12). A theoretical procedure of the determination of $\hat{\alpha}_{Tc}(n)$ in terms of the local gas phase temperature, $\hat{\alpha}_T(n)$, is described in the following.

Mean Canonical Bubble Temperature

of a Field Droplet

In the analytical estimate of a mean canonical temperature one assumes that each field droplet in the transition sphere of RND has a canonical structure, i.e., the temperature and concentration profiles are those given by

81

canonical model. Consider a canonical field droplet located at the field point, η , measured from the center of the test droplet. Let y be the radial location of an arbitrary point within the bubble of the field droplet measured from the center of the field droplet. Then, according to the result of the DIB model, the temperature distribution in the bubble of the canonical field droplet is given by

$$\alpha_T(\eta,y) = \gamma_F \left\{ \exp\left[\frac{1}{\sigma(\eta)} \left(1 - \frac{1}{y}\right) - 1\right] \right\} \tag{14}$$

where

$$\sigma = 4 \pi \rho D r_\ell(\eta)$$

Additionally, the canonical temperature, $\hat{\alpha}_{Tc}(\eta)$ is obtained by replacing y in Eq. (14) by y_c; i.e., the radius of the bubble. The result is

$$\hat{\alpha}_{Tc}(\eta) \equiv \alpha_T(\eta,y_c) = \gamma_F \left\{ \exp\left[\frac{1}{\sigma(\eta)} \left(1 - \frac{1}{y_c}\right)\right] - 1 \right\} \tag{15}$$

Since the local gas temperature $\hat{\alpha}_T(\eta)$ equals to the volume averaged mean gas temperature in the bubble of a field droplet, one writes

$$\hat{\alpha}_T(\eta) \equiv \frac{1}{V_c} \int_1^{y_c} \alpha_T(\eta,y) y \, dy \tag{16}$$

where V_c is the non-dimensional volume of the bubble given by

$$V_c = \frac{1}{3}(y_c^3 - 1)$$

In order to express $\hat{\alpha}_{Tc}(\eta)$ in terms of $\hat{\alpha}_T(\eta)$, one inroduces the correlation function λ as

$$\lambda(\eta, y_c) = \alpha_{Tc}(\eta, y_c)/\hat{\alpha}_T(\eta) \tag{17}$$

By comparing Eqs. (16) and (17), one identifies $\lambda(\eta, y_c)$ as follows

$$\lambda(\eta, y_c) = \frac{\{\exp[\frac{1}{\sigma(\eta)}(1-\frac{1}{y})-1]-1\} \ (y_c^3-1)}{3\int_1^{y_c}\{\exp[\frac{1}{\sigma(\eta)}(1-\frac{1}{y})]-1\} \ y^2 dy} \tag{18}$$

Thus, the non-dimensional vaporization rate, μ, of a field droplet is given by

$$\mu = \frac{\dot{m}(\eta)}{\dot{m}(o)} = \frac{4\pi\rho D r_\ell}{\dot{m}(o)} \ \frac{\ln\left(1+\frac{\lambda\hat{\alpha}_T}{\gamma_F}\right)}{1-\zeta_c(\eta)} \tag{19}$$

where $\zeta_c(\eta) = \zeta_{co}\theta(\eta)g(\eta)^{1/3}$ \hfill (20)

By substituting (19) into Eq. (2), for $\hat{\psi}_i = \hat{\psi}_T$, one obtains the following equation.

$$\frac{d^2\phi}{d\eta^2} + \frac{2}{\eta}\frac{d\phi}{d\eta} - G_s \ \theta g \ \frac{\ln[1-\lambda+\lambda e^\phi]}{1-\zeta_c(\eta)} = 0 \tag{21}$$

where

$$\phi = \frac{d\hat{\psi}_m}{d\eta} = \ell n\ (1 + \frac{\hat{\alpha}_T(\eta)}{\gamma_F}) \tag{22}$$

In the ensuing analysis, λ will be assumed to be unity. This corresponds to droplet vaporization with a high transfer number. The general case, $\lambda \neq 1$, can be solved by an iterative analysis with a guessed value of $\sigma(\eta)$ to calculate approximate ϕ from Eq. (21). The iteration will continue until the vaporization rate prediced from the iterative solution converages to the guessed value of σ. It is expected that the temperature rise in the radial direction is faster when $\lambda>1$. Details of the general case will be reported in the future.

The last step required for determining μ which appears in the scaling law is to determine ϕ as a function of η. With $\lambda=1$, one can show that the expression for ϕ which satisfies $\phi=\phi_{co}$ at $\eta = \eta_{co}$ and $\phi=\phi_{ts}$ at $\eta=\eta_{ts}$ is given by a linear combination of two homogeneous solutions W_1 and W_2, that satisfy the canonical boundary conditions; $W_1(\eta_{co})=1$, $\frac{dW_1}{d\eta}(\eta_{co})=0$ and $\frac{dW_2}{d\eta}(\eta_{co}) = 1$,

$$\phi(\eta) = \phi_{co}\{W_1(\eta) + [\frac{\phi_{ts}}{\phi_{co}} - W_1(\eta_{ts})]\ \frac{W_2(\eta)}{W_2(\eta_{ts})}\} \tag{23}$$

where ϕ_{co}, the characteristic value, is determined in terms of ϕ_{ts} as follows.

By equating the vaporization rate in the canonical form (5) and renormalized form (3) and by using the definition of ϕ given by Eq. (22), one obtains

$$\dot{m}(o) = \frac{4\pi\rho Dr_\ell(o)}{1-\zeta_{co}}\phi_{co} = \frac{4\pi\rho Dr_\ell(o)\ \phi_{ts}}{1-\zeta_{ts} + G_s \int_{\eta_{co}}^{\eta_{ts}} \int_{\eta_{co}}^{\eta} K(\eta|\xi)\mu(\xi)d\xi d\eta} \tag{24}$$

84

where $\mu(\xi) = \theta(\xi) \dfrac{1-\zeta_{co}}{1-\zeta_{c\eta}} \dfrac{\phi(\xi)}{\phi_{co}}$ (25)

and

$$\theta(\xi) = r_\ell(\xi)/r_{\ell o} \qquad (26)$$

On substituting the expression of $\phi(\eta)$ given by Eq. (23) into RHS of Eq. (25) and by inserting the resulting expression in the μ-term appears in the denominator of the Eq. (24), one obtains

$$\frac{\phi_{co}}{\phi_{ts}} = \frac{\Omega_{co}}{\Omega_{ts}} = \Lambda(G_s, \eta_{co}, \eta_{ts}) \qquad (27)$$

where

$$\Lambda = \frac{1-\zeta_{ts} - G_s \int_{\eta_{co}}^{\eta_{ts}} \int_{\eta_{co}}^{\eta} K(\eta|\xi)\theta(\xi)\dfrac{1-\zeta_{co}}{1-\zeta(\xi)} \dfrac{W_2(\xi)}{W_2(\eta_{ts})} \, d\xi d\eta}{1-\zeta_{ts} + G_s \int_{\eta_{co}}^{\eta_{ts}} \int_{\eta_{co}}^{\eta} K(\eta|\xi)\theta(\xi)\dfrac{1-\zeta_{co}}{1-\zeta(\xi)} [W_1(\xi) - \dfrac{W_1(\eta_{ts})}{W_2(\eta_{ts})} W_2(\xi)] d\xi d\eta} \qquad (28)$$

Finally, the scaling factor Eq. (10) can be expressed in terms of W_1 and W_2 as follows

$$c_v = \left\{ 1 - \zeta_{ts} + G_s \int_{\eta_{co}}^{\eta_{ts}} \int_{\eta_{co}}^{\eta} K(\eta|\xi)\theta(\xi) \frac{1-\zeta_{co}}{1-\zeta} [w_1(\xi) + BW_2(\xi)] d\xi d\eta \right\}^{-1}$$

where

$$B = [\frac{1}{\Lambda} - W_1(\eta_{ts})]/W_2(\eta_{ts})$$

4 Numerical Results

A numerical analysis will examine the structure and scaling laws of RND and their dependence on the principal collective interaction parameters of a stationary cloud of n-octane droplets with the following fuel properties; $\rho_\ell = 707$ Kg/m^3 $T_b = 398.7$ k, L = 71.7 Kcal/Kg, and $W_F = 114.14$ Kg/kg-mole.

(1) Pair-Distribution Function and Canonical Bubble

In the absence of experimental data, a pair-distribution function is constructed on the basis of the geometrical distribution of molecules in a dense liquid. The following two parameter function is adopted for the numerical calculation.

$$g(\eta) = 1 + a \exp(-b\eta) \cos(2\pi\eta_{co}), \qquad 2\eta_{co} < \eta \leq \eta_{ts} \qquad (29)$$

where a and b are constants to be determined from the experimental data. In the present analysis a = 1.8, b = 0.65 are chosen. The resulting distribution patterns are shown in Fig. 3. The corresponding signatures of the inverse of the radius of canonical bubbles with $\eta_{co} = 5$, 10, and 15 are shown in Fig. 4.

(2) Vaporization Shape Factor

A pronounced increase of μ in the radial direction is observed for a smaller value of droplet spacing, i.e. $\eta_{co} = 7.5$ in Fig. 5. The ratio of the vaporization rate of the droplet located at the first coordination shell, for

the case of η_{co} = 7.5, is approximately 5% of the corresponding value of RND with η_{co} = 15. This trend of a higher increasing rate of μ at smaller canonical bubble radii, or droplet spacing, is a common feature for small droplet spacing. This is confirmed for the cases characterized by pair-distribution functions with different values of a and b. The results suggest that "μ -stratification" is a unique feature of RND in non-dilute clouds or spray.

(3) Temperature Distribution

High μ- stratification at smaller droplet spacing, as illustrated in Fig. 5 is due to the steep radial temperature gradients in the transition sphere, shown in Fig. (6). Indeed, the comparison of "μ- T stratifications" suggest that (1) the rapid vaporization in outer layer of the cloud collectively quench the environment and thereby reduce the vaporization of the test droplet and (2) the increase in η_{ts} at a fixed droplet spacing tends to reduce the inward heat transfer rate and thus suppresses the vaporization of the test droplet.

(4) Vaporization Rate - Correction Factor

The correction factors of RNDs for three selected values of η_{co}, Fig. 7, are found to decrease monotonically as the group combustion number of RND increases. Saturation is projected to occur when G_{RN}=30~40 with η_{co}= 7.5. While the group combustion number is a primary factor controlling the magnitude of C_v, Fig. 7 shows a small variation in the correction factor for two RND's which have the same group combustion number but different renormalization number, $\beta = \eta_{ts}/\eta_{co}$.

4   Discussion

Scaling Law with Linear Stratification Model

In order to facilitate the practical application of the scaling law, the correction factor is integrated by adopting the following functional form of g_μ

$$g_\mu = \overline{g_\mu} K_1 \eta$$

where K_1 is a stratification coefficient, and $\overline{g_\mu}$ is the mean value of the weighted vaporization shape factor. The correction factor predicted by the linear stratification model described above, is given by

$$C_v = \{ 1 - \zeta_{ts} + G_{RN} [(1 - \frac{1}{\beta})(1 + \frac{1}{\beta} - \frac{2}{\beta^2}) + \frac{1}{2} K_1 \eta_{ts} (1 - \frac{1}{\beta})(1 + \frac{1}{\beta} + \frac{1}{\beta^2} - \frac{1}{\beta^3})] \} \quad (30)$$

where $G_{RN} = \frac{1}{6} G_s \eta_{ts}^2 \overline{g_\mu}$.

SPRAY CLASSIFICATION

Numerical assessment of the scaling law suggests the following structural classification of non-dilute sprays.

1.   Diffusively Dense Cloud

In a moderately dense cloud, RND is expected to have a large transition sphere that has no μ- stratification. The reduction in the vaporization is attributed to uniform thermal quenching. The correction factor given below is described by the group combustion alone:

$$C_v = (1 + G_{RN})^{-1} \quad\quad\quad (31)$$

88

C-2

2. Densely Stratified Cloud

This cloud is featured with a strong stratification in a transition sphere that causes an intense collective quenching and a reduction in the vaporization rate of the test droplet. The renormalization number η_{ts}/η_{co} is larger than unity so that the correction factor is given by

$$C_v = [1 - \zeta_{ts} + G_{RN}(1 + \frac{1}{2} K_1 \eta_{ts})]^{-1} \tag{32}$$

3. Sharply Dense Cloud - Fine Structure

When the coordination shells contain the largest possible number of the droplet so that the renormalization number is not excessively large compared with unity, the correction factor depends on all the collective parameters: G_{RN}, η_{ts}/η_{co} and η_{ts}. Two sharply dense clouds with the same group combustion number will exhibit structural variation when the renormalization number is different.

5   Conclusion

The present theory portrays a droplet interacting with its neighbors by a minimum sized "dressed" droplet structured with a centrally located droplet and its bubble, e.g. Droplet-in-Bubble, surrounded by a quasi-droplet cloud spreading through a transition sphere. The distribution of quasi-droplets and the size of the cloud are described by a pair distribution function. The introduction of the transition sphere and the correspondence hypothesis postulating the equivalence between the average gas properties on the transition sphere with the gas properties of the continuum flow field, as the limit R_{ts}/L goes to zero, constitutes the fundamental link between the discrete droplet dominated region with that of the surrounding continuum

flow.   This feature provides the basis of the theory of short-range interaction and droplet rate processes.

The vaporization scaling law reveals that the droplet vaporization is retarded primarily by the collective thermal quenching and the formation of high vapor concentration in the transition sphere.   The retardation is scaled by combined topological-thermochemical parameters: the group combustion number, renormalization number and droplet spacing.   The scaling laws suggest that non-dilute clouds or sprays can be classified into: (1) "Diffusively Dense" clouds in which the vaporization reduction is attributed to the effects of uniform thermal quenching that can be scaled by the group combustion number alone; (2) "Densely Stratified" clouds, with marked radial stratification due to the large temperature gradient which exists in the transition sphere; and (3) "Sharply Dense" clouds, with a relatively large canonical bubble, and radial stratification so that the scaling law depends on G_{RN}, n_{ts} and β. Selected case studies show that the correction factor falls monotonically as the group combustion number increases and the saturation is expected to occur when the G_{RN} is of the order of $30 \sim 40$, with the droplet spacing of approximately 7.5 times of the droplet size and environment temperature of 500 K.

Finally, the validity of quasi-steady (Q-S) approximation is examined by comparing the relative magnitude of the characteristic time, $t_{diff.}$, of difusion through the transition sphere and the life time, t_{life}, of RND.   By adopting the renormalized vaporization laws, Eqs. (8) and (10), and a standard diffusion time for the transition sphere of RND, one concludes that the Q-S approximation is valid when the following inequality is satisfied

$$\frac{t_{dif.}}{t_{life}} = 2C_v \eta_{ts}^2 \frac{\rho}{\rho_\ell} \ell_n(1 + B) \qquad (33)$$

where $B = C_p(T-T_b)/L$.

With $\rho_\ell \sim 10^3 \text{kg/m}^3$, $\rho \sim 1 \text{ kg/n}^3$, $T-T_b \sim 100^0 \text{ K}$ $L \sim 10^2 \text{Kcal/kg}$, $C_p \sim 0.5$ Kcal/Kg-K the numerical values of $\frac{t_{diff}}{t_{lifℓ}}$ is 5×10^{-4}.

Alternatively, by using the asymptotic form of C_v for high G_{RN}, deduced from Eq. (30), i.e., $c_v \sim G_{RN}^{-1} = (\frac{1}{6} G_s \eta_{ts} g\mu)^{-1}$, one transforms Eq. (33) into the following form

$$\overline{g\mu} G_s >> G_s^* \qquad (34)$$

where $G_s^* = 12 \frac{\rho}{\rho_\ell} \ln(1 + B)$

Recalling that $G_s = 4\pi \eta r_{\ell o}^3$ is equal to a third of the void fraction, and $\overline{g\mu} \sim 0(1)$, one concludes that the Q-S approximation is valid in high G-sprays when the void fraction exceeds a third of the values of G_s^*. For typical values of ρ_ℓ, ρ, $T-T_b$, C_p and L given above, Eq. (34) reduces to

$$nr_{\ell o}^3 >> 4 \times 10^{-4} \qquad (35)$$

For example, with SMD=100μ , the Q-S approximation is valid when n is greater than 3200 drops/cc, whereas for SMD=200μ, the corresponding number density is 400 drops/cc.

The criterion (33) or its alternative form can be encoded in a spray numerical code to test the validity of Q-S assumption at each point of a spray

flow field. When the approximation is invalid, an alternative transient droplet laws should be used to determine the interfacial processes. Note that such droplet transient processes should be able to predict the change in the nature of interfacial processes. For example, a vaporizing droplet may reach the state of saturation when the droplet spacing falls below the critical value or when the thermal shielding retards the heat flux to the droplet.

REFERENCES

1. Chiu, H.H. and Liu, T.M.: <u>COMB. SCI. AND TECH.</u>, 17, 127, 1(1977).

2. Labowsky, M. and Rosner, D.E., Advances in Chemistry Series No 166 Amer. Chem. Soc., (1978).

3. Twardus, E.M., and Brzustowski, T.A.: Comb. Sci. Tech 17, 215, (1978).

4. Tishkoff, J.M.: Int. J. Heat and Mass Transfer 22, 1407, (1979).

5. Labowsky, M.: Combust. Sci. Tech. 22, 127, (1980).

6. Umemura, A.: Eighteenth Symposium (International) on Combustion, 1335, The Combustion Institute, 1981.

7. Chiu, H.H., Kim, H.Y., and Croke, E.J.: Nineteenth Symposium (International) on Combustion, 971, The Combustion Institute, 1982.

8. Bellan, J. and Cuffel, R.: Combust. Flame 51, 55, (1983).

9. Sirignano, W.A.: Prog. Energy Combust. Sci. 9, 291, (1983).

10. Sichel, M. and Panlaniswamy, S.: Twentieth Symposium (International) on Combustion, 1789, The Combustion Institute, 1984.

11. Chiu, H.H.: "Theory of Bipropellant Combustion, Part I – Conjugate, Normal and Composite Combustion Phenomena:" AIAA-86-0220 Presented at the AIAA 24TH Aerospace Sciences Meeting, Reno, Nevada, 1986.

12. Chiu, H.H.: "Theory of Renormalized Droplets I Law of Droplet Vaporization Rate Under Short-Range Droplet Interaction" Presented at First Annual Conference on Liquid Atomization and Spray Systems ILASS Americas, Madison, Wisconsin, 1987.

13. Jang, S.D. and Chiu, H.H.: "Theory of Renormalized Droplets, II, Nonsteady Vaporization Droplet in Non-Dilute Sprays" AIAA-88-0639, Presented at the AIAA 26TH Aerospace Sciences Meeting, Reno Nevada, 1988.

14. McCreath, C.G. and Chigier, N.A.: Fourteenth Symposium (International) on Combustion, 1355, The Combustion Institute, 1973.

15. Miyasaka, K. and Law, C.K.: Eighteenth Symposium (International) on Combustion, 283, The Combustion Institute, 1981.

16. Yule, A.J. and Bolado: Combust Flame 55, 1, (1984).

17. Xiong, T.Y., Law, C.K. and Miyasaka, K.: Twentieth Symposium (International) on Combustion, 1781, The Combustion Institute, 1984.

18. Roshland, C.P. and Bowman, C.T.: Twentieth Symposium (International) on Combustion, 1979, The Combustion Institute, 1984.
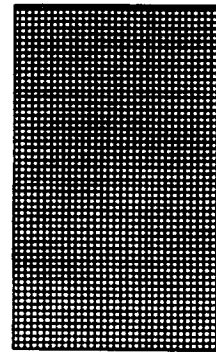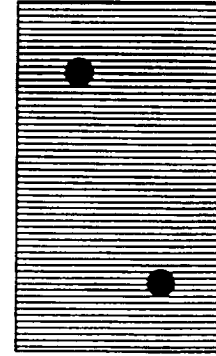
ELEMENTAL DROPLET MODELS
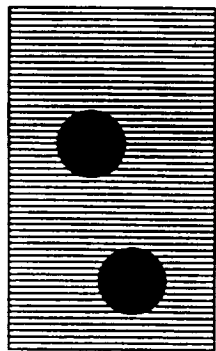
Natural
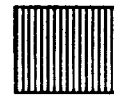Droplet Model
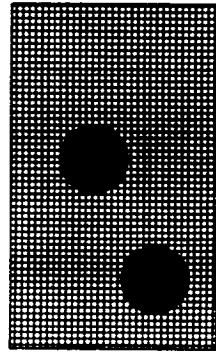
Non-Uniformly
Smeared
Droplet Model

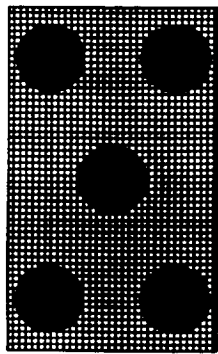Uniformly
Smeared Two
Droplet Model

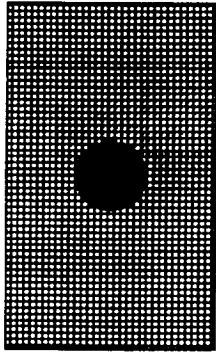Point Source
Droplet Model

Gas Phase

Smeared Liquid Phase

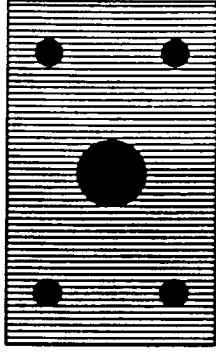Fig. 1 Droplet Models; Elemental Droplets

94

COMPOSITE DROPLET MODELS

Natural Droplet
and Non-Uniformly
Smeared Droplets

Natural Droplet
and Uniformly
Smeared Droplets

Natural Droplet
and Point
Source Droplets

Gas Phase

Smeared Liquid Phase

Fig. 1   Droplet Model; Composite Droplet
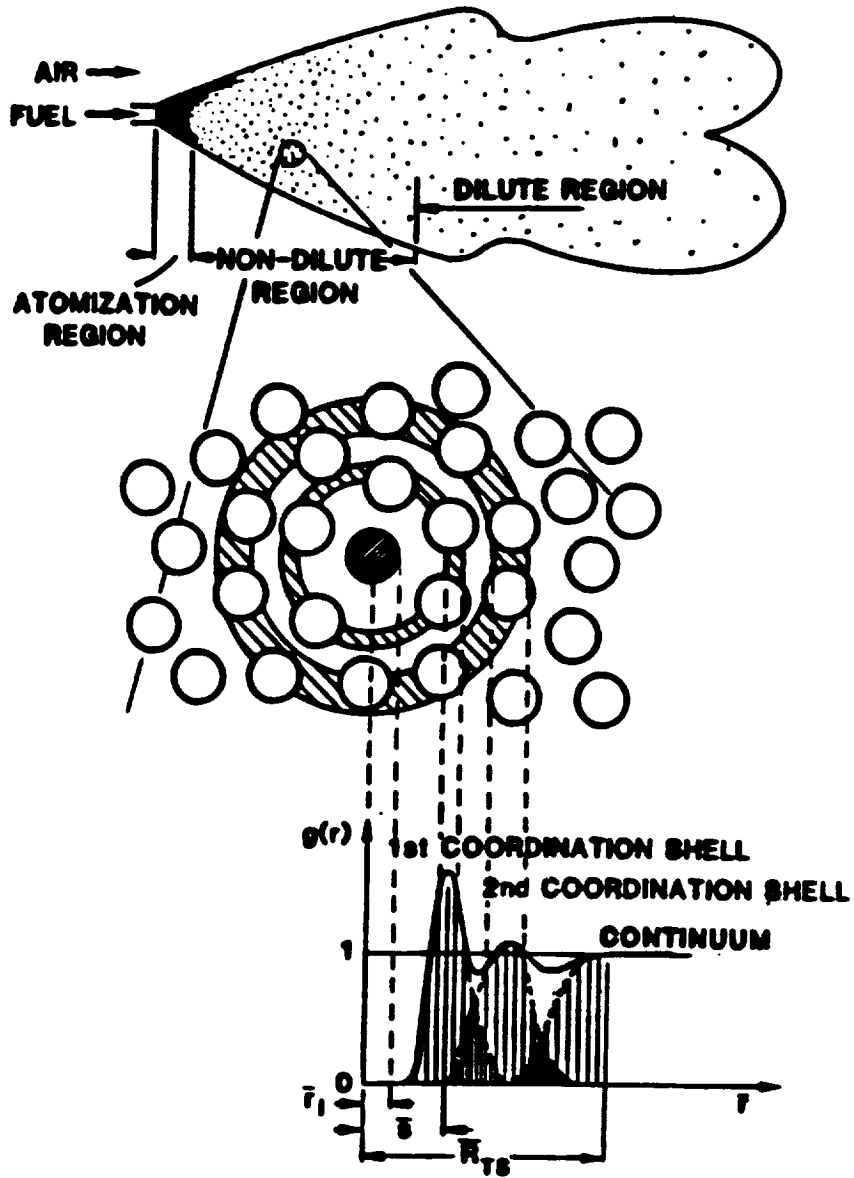
FIG. 2 Structure of renormalized droplet in non-dilute spray and the schematic of quasi-droplet cloud in transition sphere.
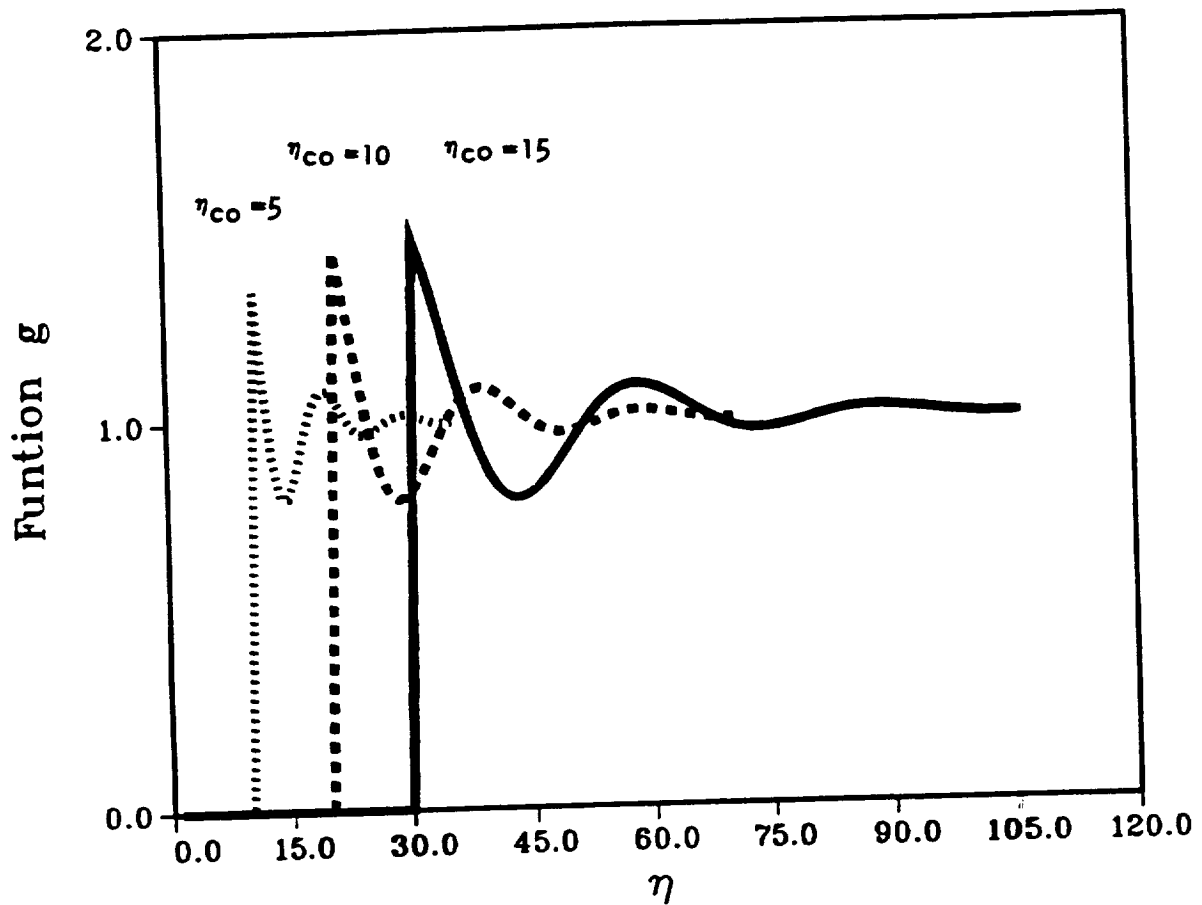
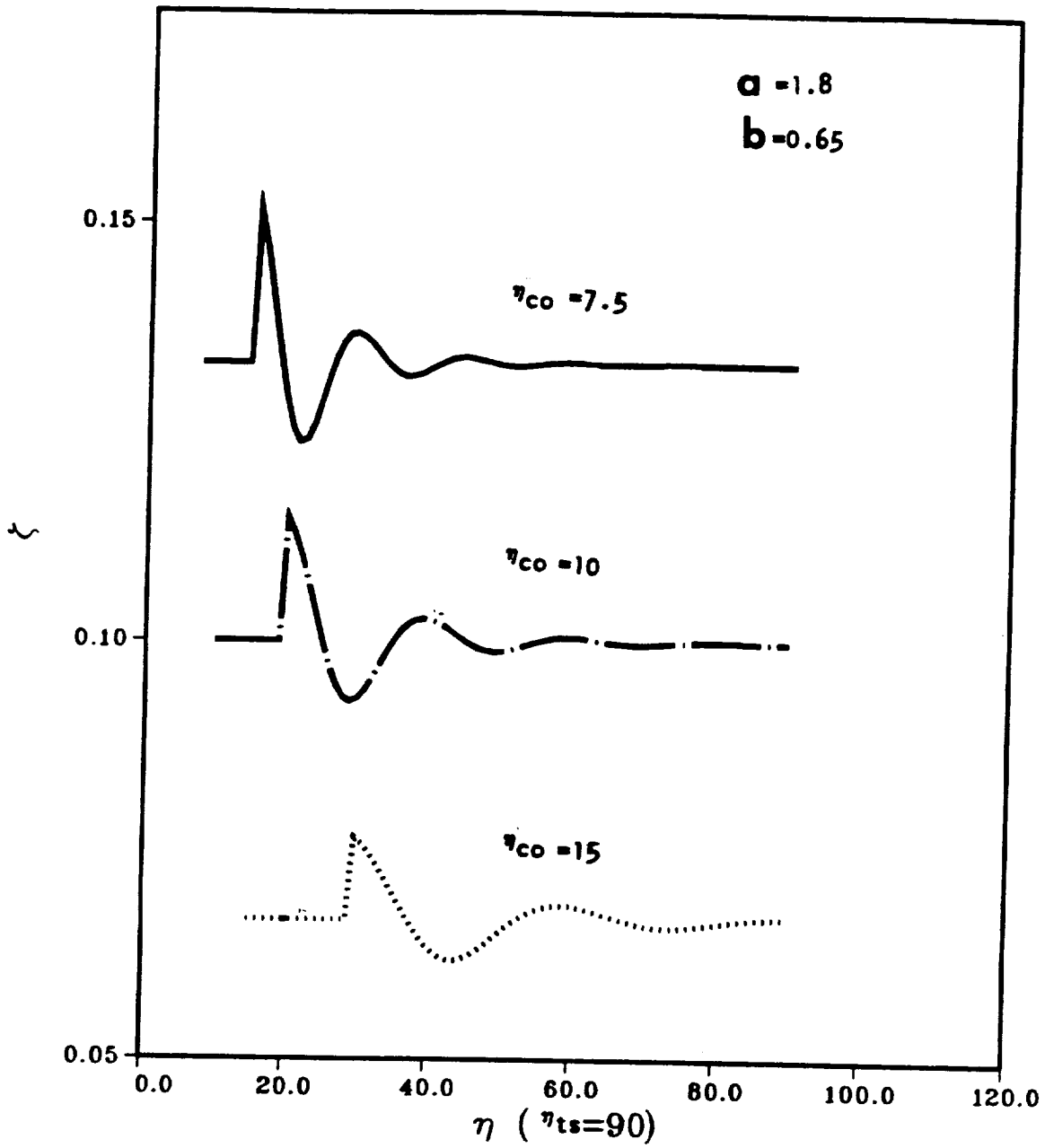Fig. 3 Pair-distribution function of quasi-droplets in transition sphere for three selected test droplet bubble sizes.

Fig. 4 Signature of the inverse of cannonical bubble radius
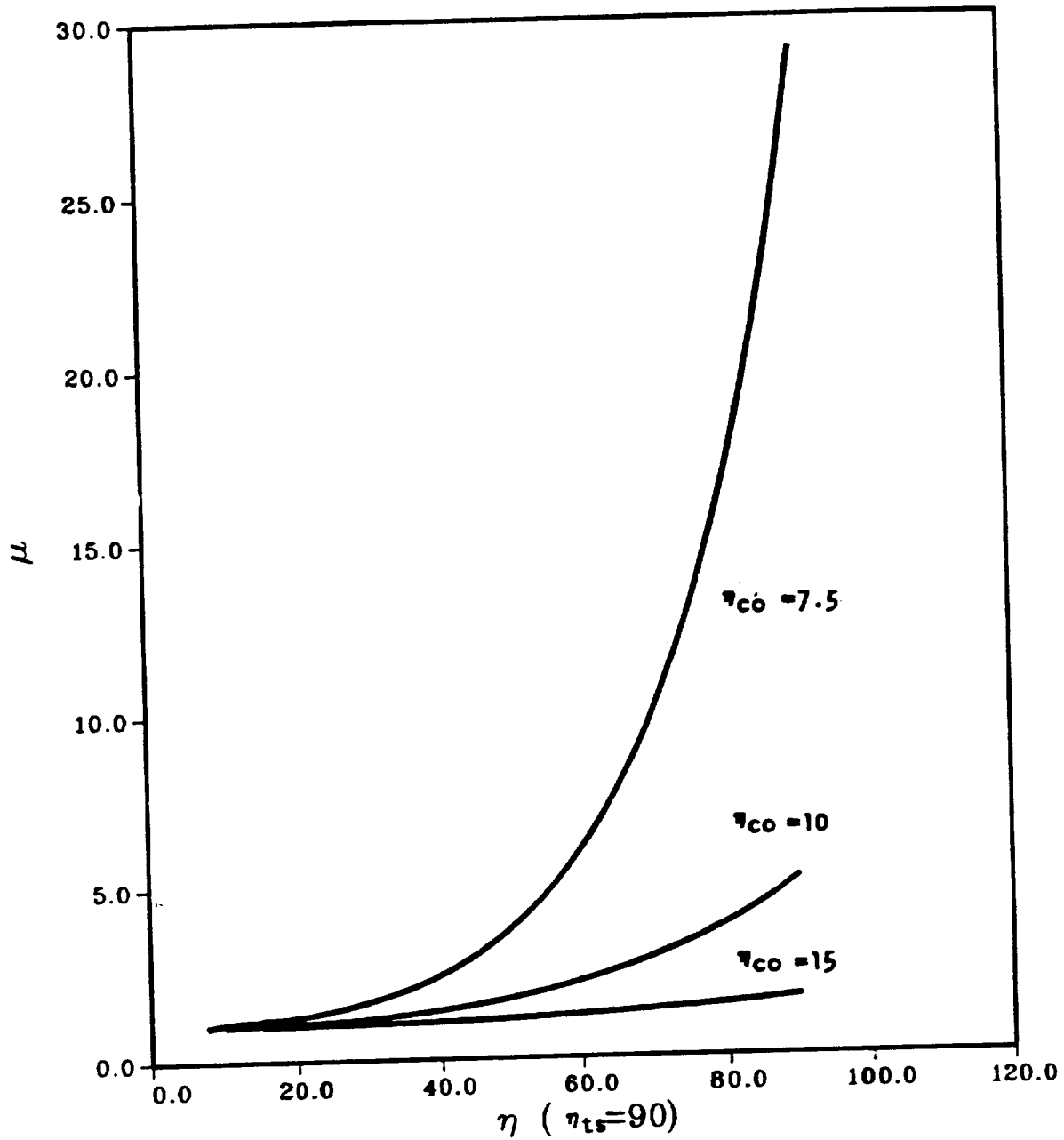for three selected test droplet bubble sizes.

98

Fig. 5   μ-stratification; Vaporization shape factor distribution in transition sphere for three selected test droplet bubble sizes.
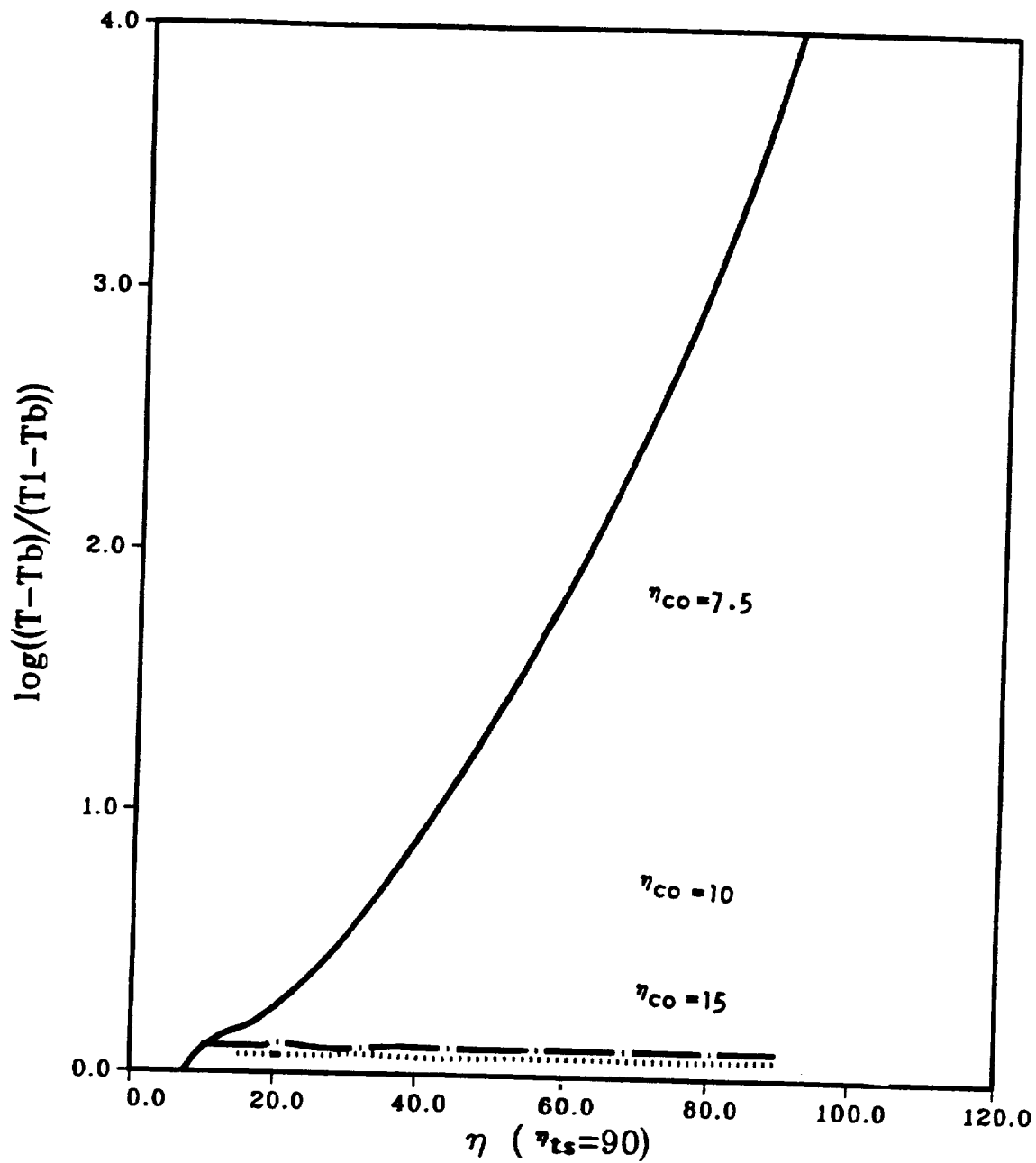
Fig. 6   T-stratification = gas temperature distribution in transition sphere for three selected test droplet bubble sizes.
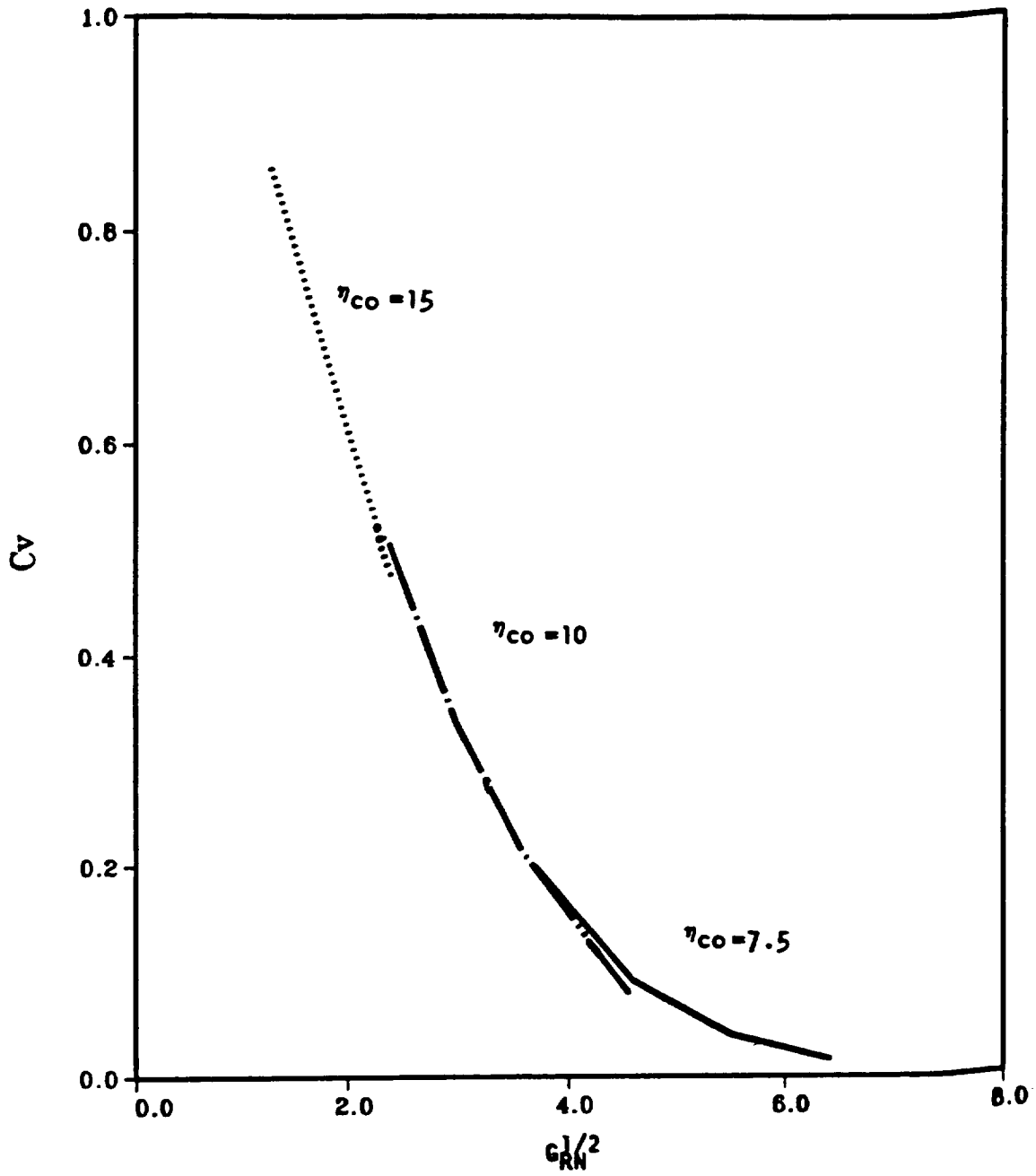
Fig. 7 Correction factor for vaporization rate vs group com-
bustion number for three selected test droplet sizes
Exact Solution.